

## VLBA DETERMINATION OF THE DISTANCE TO NEARBY STAR-FORMING REGIONS. I. THE DISTANCE TO T TAURI WITH 0.4% ACCURACY

LAURENT LOINARD AND ROSA M. TORRES

Centro de Radioastronomía y Astrofísica, Universidad Nacional Autónoma de México, Apartado Postal 72-3 (Xangari), 58089 Morelia, Michoacán, Mexico; lloinard@astrosmo.unam.mx

AMY J. MIODUSZEWSKI

National Radio Astronomy Observatory, Array Operations Center, 1003 Lopezville Road, Socorro, NM 87801

LUIS F. RODRÍGUEZ, ROSA A. GONZÁLEZ-LÓPEZLIRA, AND RÉGIS LACHAUME

Centro de Radioastronomía y Astrofísica, Universidad Nacional Autónoma de México, Apartado Postal 72-3 (Xangari), 58089 Morelia, Michoacán, Mexico

AND

VIRGILIO VÁZQUEZ AND ERANDY GONZÁLEZ

Universidad Tecnológica de la Mixteca, Carretera Huajuapán-Acatlilma, 69000 Huajuapán de León, Oaxaca, Mexico

Received 2007 June 25; accepted 2007 August 7

### ABSTRACT

In this article, we present the results of a series of 12 3.6 cm radio continuum observations of T Tau Sb, one of the companions of the famous young stellar object T Tauri. The data were collected roughly every 2 months between 2003 September and 2005 July with the Very Long Baseline Array (VLBA). Thanks to the remarkably accurate astrometry delivered by the VLBA, the absolute position of T Tau Sb could be measured with a precision typically better than about  $100 \mu\text{as}$  at each of the 12 observed epochs. The trajectory of T Tau Sb on the plane of the sky could therefore be traced very precisely and was modeled as the superposition of the trigonometric parallax of the source and an accelerated proper motion. The best fit yields a distance to T Tau Sb of  $147.6 \pm 0.6$  pc. The observed positions of T Tau Sb are in good agreement with recent infrared measurements, but they seem to favor a somewhat longer orbital period than that recently reported by Duchêne and coworkers for the T Tau Sa/T Tau Sb system.

*Subject headings:* astrometry — binaries: general — magnetic fields — radiation mechanisms: nonthermal — radio continuum: stars — stars: formation

### 1. INTRODUCTION

To provide accurate observational constraints for pre-main-sequence evolutionary models and thereby improve our understanding of star formation, it is crucial to measure the properties (age, mass, luminosity, etc.) of individual young stars as accurately as possible. The determination of most of these parameters, however, depends critically on the often poorly known distance to the object under consideration. While the average distance to nearby low-mass star-forming regions (e.g., Taurus or Ophiuchus) has been estimated to about 20% precision using indirect methods (Elias 1978a, 1978b; Kenyon et al. 1994; Knude & Høg 1998), the line-of-sight depth of these regions is largely unknown, and accurate distances to individual objects are still missing. Even the highly successful *Hipparcos* mission (Perryman et al. 1997) did little to improve the situation (Bertout et al. 1999), because young stars are still heavily embedded in their parental clouds and are therefore faint in the optical bands observed by *Hipparcos*. Future space missions such as *Gaia* will undoubtedly have the capacity to accurately measure the trigonometric parallax of optically fainter stars, but these missions will still be unable to access very deeply embedded sources, and they will only start to provide results in about a decade. In the meantime, extremely high quality infrared and X-ray surveys of many star-forming regions are being obtained (e.g., Evans et al. 2003; Güdel et al. 2007), and their potential cannot be fully exploited because of the unavailability of good distance estimates.

Low-mass young stars often generate nonthermal continuum emission produced by the interaction of free electrons with the

intense magnetic fields that tend to exist near their surfaces (e.g., Feigelson & Montmerle 1999). Since the magnetic field strength decreases quickly with the distance to the stellar surface (as  $r^{-3}$  in the magnetic dipole approximation), the emission is strongly concentrated to the inner few stellar radii. If the magnetic field intensity and the electron energy are sufficient, the resulting compact radio emission can be detected with very long baseline interferometry (VLBI; e.g., André et al. 1992). The relatively recent possibility of accurately calibrating the phase of VLBI observations of faint, compact radio sources using nearby quasars makes it possible to measure the absolute position of these objects (or, more precisely, the angular offset between them and the calibrating quasar) to better than a tenth of a milliarcsecond (Loinard et al. 2005; see also below). This level of precision is sufficient to constrain the trigonometric parallax of sources within a few hundred parsecs of the Sun (in particular, of nearby young stars) with a precision of better than a few percent using multiepoch VLBI observations.

Taking advantage of this situation, we have recently initiated a large project aimed at accurately measuring the trigonometric parallax of a significant sample of magnetically active young stars in nearby star-forming regions (Taurus, Ophiuchus, Perseus, Serpens, and Cepheus) using the 10 element Very Long Baseline Array (VLBA) of the National Radio Astronomy Observatory (NRAO). In the present article, we concentrate on T Tau Sb, one of the members of the famous young stellar system T Tauri (see, e.g., Duchêne et al. [2006] for a recent summary of the properties of that system). T Tau Sb has long been known to be associated with a compact nonthermal radio source (Skinner & Brown

TABLE 1  
 SOURCE POSITION AND FLUX

Mean UT Date (yyyy.mm.dd hh:mm) (1)	$\alpha$ (J2000.0) (2)	$\sigma_\alpha$ (s) (3)	$\delta$ (J2000.0) (4)	$\sigma_\delta$ (arcsec) (5)	$F_\nu$ (mJy) (6)	$\sigma$ ( $\mu$ Jy) (7)
2003.09.24 11:33 .....	04 21 59.4252942	0.0000013	19 32 05.717618	0.000043	1.62	74
2003.11.18 08:02 .....	04 21 59.4249805	0.0000015	19 32 05.716554	0.000043	1.74	66
2004.01.15 04:09 .....	04 21 59.4245823	0.0000036	19 32 05.715322	0.000108	0.92	72
2004.03.26 23:26 .....	04 21 59.4245420	0.0000017	19 32 05.715333	0.000050	1.27	70
2004.05.13 20:17 .....	04 21 59.4248818	0.0000016	19 32 05.716034	0.000055	1.90	111
2004.07.08 16:37 .....	04 21 59.4253464	0.0000020	19 32 05.716652	0.000058	1.25	64
2004.09.16 11:59 .....	04 21 59.4255476	0.0000015	19 32 05.716602	0.000042	1.61	70
2004.11.09 08:27 .....	04 21 59.4252999	0.0000015	19 32 05.715631	0.000039	3.36	104
2004.12.28 05:14 .....	04 21 59.4249488	0.0000015	19 32 05.714344	0.000050	1.26	70
2005.02.24 01:26 .....	04 21 59.4247667	0.0000016	19 32 05.713826	0.000042	2.30	80
2005.05.09 20:32 .....	04 21 59.4251475	0.0000060	19 32 05.714852	0.000182	1.12	106
2005.07.08 16:36 .....	04 21 59.4256679	0.0000019	19 32 05.715598	0.000060	1.41	75

NOTE.—Units of right ascension are hours, minutes, and seconds, and units of declination are degrees, arcminutes, and arcseconds.

1994; Phillips et al. 1993; Johnston et al. 2003) characterized by strong variability and significant circular polarization. An extended thermal radio halo studied in detail by Loinard et al. (2007) and probably related to stellar winds also exists around T Tau Sb. While this extended structure contributes to the total radio flux as measured, for instance, with the VLA, it is effectively filtered out in VLBI experiments. Indeed, in the intercontinental VLBI observations published by Smith et al. (2003), only about 40% of the simultaneously measured VLA flux density is retrieved. The radio source detected by Smith et al. (2003) is very compact ( $R < 15 R_\odot$ ), and its flux was about 3 mJy at the time of their observations. Its trajectory over the plane of the sky was studied by Loinard et al. (2005) using a series of seven VLBA observations. Unfortunately, these data were recently found to have been affected by a bug that caused the VLBA correlator to use the predicted rather than measured Earth Orientation Parameters (EOPs).<sup>1</sup> This problem corrupted the visibility phases and strongly affected the quality of the astrometry of the data published in Loinard et al. (2005). The postfit rms for the Loinard et al. (2005) data was about 250 mas, compared with 60–90 mas for the present data (see below). Here we reanalyze these VLBA data and combine them with five newer observations to measure the trigonometric parallax and study the proper motion of T Tau Sb.

## 2. OBSERVATIONS AND DATA CALIBRATION

In this paper, we make use of a series of 12 continuum 3.6 cm (8.42 GHz) observations of T Tau Sb obtained every 2 months between 2003 September and 2005 July with the VLBA (Table 1). Our phase center was at  $\alpha_{J2000.0} = 04^{\text{h}}21^{\text{m}}59.4263^{\text{s}}$ ,  $\delta_{J2000.0} = +19^\circ 32' 05.730''$ , which is the position of the compact source detected by Smith et al. (2003). Each observation consisted of a series of cycles with 2 minutes spent on-source and 1 minute spent on the main phase-referencing quasar J0428+1732, located  $2.6^\circ$  away. J0428+1732 is a very compact extragalactic source whose absolute position ( $\alpha_{J2000.0} = 04^{\text{h}}28^{\text{m}}35.633679^{\text{s}}$ ,  $\delta_{J2000.0} = 17^\circ 32' 23.58799''$ ) is known to better than 1 mas ( $\sigma_\alpha = 0.59$  mas,  $\sigma_\delta = 0.89$  mas; Beasley et al. 2002). During the first six observations, the secondary quasar J0431+1731 was also observed periodically, about every 30 minutes, both to check the astrometric quality of the data and to enable us to compare our results with those of Smith et al. (2003), who used J0431+1731 as their phase calibrator. A detailed comparison with the results

of Smith et al. (2003) and with the numerous VLA observations available from the literature, however, will be postponed to a forthcoming article.

The data were edited and calibrated using the Astronomical Image Processing System (AIPS; Greisen 2003). The basic data reduction followed the standard VLBA procedures for phase-referenced observations. First, the most accurate measured EOPs obtained from the US Naval Observatory database were applied to the data in order to correct the erroneous values initially used by the VLBA correlator. Second, we accounted for dispersive delays caused by free electrons in the Earth's atmosphere, using an estimate of the electron content of the ionosphere derived from Global Positioning System (GPS) measurements. An a priori amplitude calibration based on the measured system temperatures and standard gain curves was then applied. The fourth step was to correct the phases for antenna parallactic angle effects, and the fifth was to remove residual instrumental delays caused by the VLBA electronics. This was done by measuring the delays and phase residuals for each antenna and IF, using the fringes obtained on a strong calibrator. The final step of this initial calibration was to remove global frequency- and time-dependent phase errors by using a global fringe-fitting procedure on the main phase calibrator (J0428+1732), which was assumed at this stage to be a point source.

In this initial calibration, the solutions from the global fringe fit were only applied to the main phase calibrator itself. The corresponding calibrated visibilities were then imaged, and several passes of self-calibration were performed to improve the overall amplitude and phase calibration. In the image obtained after the self-calibration iterations, the main phase calibrator was found to be slightly extended. To take this into account, the final global fringe-fitting part of the reduction was repeated, this time using the image of the main phase calibrator as a model instead of assuming it to be a point source. Note that a different phase calibrator model was produced for each epoch in order to account for possible small changes in the main calibrator structure from epoch to epoch. The solutions obtained after repeating this final step were edited for bad points and applied to the target source. Using an image model for the calibrator rather than assuming a point source improved the position accuracy by a few tens of microseconds.

Because of the significant overheads that were necessary to properly calibrate the data, only about 3 of the 6 hr of telescope time allocated to each of our observations were actually spent on-source. Once calibrated, the visibilities were imaged with a

<sup>1</sup> See <http://www.vlba.nrao.edu/astro/messages/eop/>.

TABLE 2  
JULIAN DATES AND EARTH COORDINATES

MEAN UT DATE (yyyy.mm.dd hh:mm)	JULIAN DATE	EARTH BARYCENTRIC COORDINATES (AU)		
		<i>X</i>	<i>Y</i>	<i>Z</i>
2003.09.24 11:33 .....	2,452,906.981522	+1.006064570	+0.012414145	+0.005329883
2003.11.18 08:02 .....	2,452,961.834705	+0.563031813	+0.744728145	+0.322808936
2004.01.15 04:09 .....	2,453,019.672980	-0.401044530	+0.820090543	+0.355473794
2004.03.26 23:26 .....	2,453,091.476395	-0.987542097	-0.107099184	-0.046513144
2004.05.13 20:17 .....	2,453,139.345324	-0.599629779	-0.745571223	-0.323319720
2004.07.08 16:37 .....	2,453,195.192419	+0.297481514	-0.894474582	-0.387883413
2004.09.16 11:59 .....	2,453,264.999583	+1.003677539	-0.099008512	-0.043027999
2004.11.09 08:27 .....	2,453,318.852141	+0.676914299	+0.666368259	+0.288787192
2004.12.28 05:14 .....	2,453,367.718351	-0.111308860	+0.895710071	+0.388210192
2005.02.24 01:26 .....	2,453,425.559664	-0.896015668	+0.377089952	+0.163364585
2005.05.09 20:32 .....	2,453,500.355214	-0.655044089	-0.701050689	-0.304055855
2005.07.08 16:36 .....	2,453,560.191348	+0.293538593	-0.893249243	-0.387385193

pixel size of 50  $\mu$ as after weights intermediate between natural and uniform (ROBUST = 0 in AIPS) were applied. This resulted in a typical rms noise level of 70  $\mu$ Jy for most observations, although for a few epochs with less favorable weather conditions, the noise level exceeded 100  $\mu$ Jy (Table 1). T Tau Sb was detected with a signal-to-noise ratio of better than 10 at each epoch (Table 1), and its absolute position (listed in cols. [2] and [4] of Table 1) was determined using a two-dimensional Gaussian fitting procedure (task JMFIT in AIPS). This task provides an estimate of the position error (cols. [3] and [5] of Table 1) based on the expected theoretical astrometric precision of an interferometer (Condon 1997). Systematic errors, however, usually limit the actual precision of VLBI astrometry to several times this theoretical value (e.g., Fomalont 1999; Pradel et al. 2006). At the frequency of the present observations, the main sources of systematic errors are inaccuracies in the troposphere model used, as well as clock, antenna, and a priori source position errors. These effects combine to produce a systematic phase difference between the calibrator and the target that limits the precision with which the target position can be determined. We did not attempt to correct for these systematic effects here and will therefore assume that the true error on each measurement is the quadratic sum of the random error listed in Table 1 and a systematic contribution. The latter is difficult to estimate a priori and will be deduced from the fits to the data.

### 3. ASTROMETRY FITS

The displacement of T Tau Sb on the celestial sphere is the combination of its trigonometric parallax ( $\pi$ ) and its proper motion. For isolated sources, it is common to consider linear and uniform proper motions, so the right ascension ( $\alpha$ ) and the declination ( $\delta$ ) vary as a function of time  $t$  as

$$\alpha(t) = \alpha_0 + (\mu_\alpha \cos \delta)t + \pi f_\alpha(t), \quad (1)$$

$$\delta(t) = \delta_0 + \mu_\delta t + \pi f_\delta(t), \quad (2)$$

where  $\alpha_0$  and  $\delta_0$  are the coordinates of the source at a given reference epoch,  $\mu_\alpha$  and  $\mu_\delta$  are the components of the proper motion, and  $f_\alpha$  and  $f_\delta$  are the projections over  $\alpha$  and  $\delta$ , respectively, of the parallactic ellipse. The latter functions are given by (e.g., Seidelman & Fukushima 1992)

$$f_\alpha(t) = (X \sin \alpha_1 - Y \cos \alpha_1)/15 \cos \delta_1, \quad (3)$$

$$f_\delta(t) = X \cos \alpha_1 \sin \delta_1 + Y \sin \alpha_1 \sin \delta_1 - Z \cos \delta_1, \quad (4)$$

where ( $X, Y, Z$ ) are the barycentric coordinates of the Earth in units of AU, and where  $\alpha_1 = \alpha - \pi f_\alpha(t)$  and  $\delta_1 = \delta - \pi f_\delta(t)$  are the coordinates of the barycentric place of the source at each epoch. Note that  $f_\alpha$  and  $f_\delta$  depend implicitly on time (through  $X, Y$ , and  $Z$ ) and explicitly on the coordinates of the source. The latter dependence on  $\alpha_1$  and  $\delta_1$  (which are only known if the trigonometric parallax is known) implies that the fitting procedure must be iterative. The barycentric coordinates of the Earth (as well as the Julian date of each observation) were calculated using the Multiyear Interactive Computer Almanac (MICA), which was distributed as a CD-ROM by the US Naval Observatory. They are given explicitly in Table 2 for all epochs.

As mentioned earlier, T Tau Sb is a member of a multiple system (e.g., Loinard et al. 2003; Duchêne et al. 2006 and references therein), so its proper motion is likely to be affected by the gravitational influence of the other members of the system. As a consequence, the motion is likely to be curved and accelerated rather than linear and uniform. To take this into account, we have also made fits to the data that include acceleration terms. This leads to functions of the form

$$\alpha(t) = \alpha_0 + (\mu_{\alpha 0} \cos \delta)t + \frac{1}{2}(a_\alpha \cos \delta)t^2 + \pi f_\alpha(t), \quad (5)$$

$$\delta(t) = \delta_0 + \mu_{\delta 0}t + \frac{1}{2}a_\delta t^2 + \pi f_\delta(t), \quad (6)$$

where  $\mu_{\alpha 0}$  and  $\mu_{\delta 0}$  are the proper motions at a reference epoch and  $a_\alpha$  and  $a_\delta$  are the projections of the uniform acceleration. Note that the acceleration undergone by a body in Keplerian orbit is usually not uniform. Assuming a uniform acceleration is acceptable here, however, because our data cover only a small portion ( $\sim 2$  yr) of the orbital period (a few decades; Duchêne et al. 2006) of T Tau Sb. If VLBA data are obtained regularly in the next few decades, a full orbital fit will become possible, and indeed necessary.

The astrometric parameters were determined by least-squares-fitting the data points with either equations (1) and (2) or equations (5) and (6), using a singular value decomposition (SVD) scheme (see the Appendix for details). To check our results, we also performed two other fits to the data: a linear one based on the associated normal equations, and a nonlinear one based on the Levenberg-Marquardt algorithm. They gave results identical to those

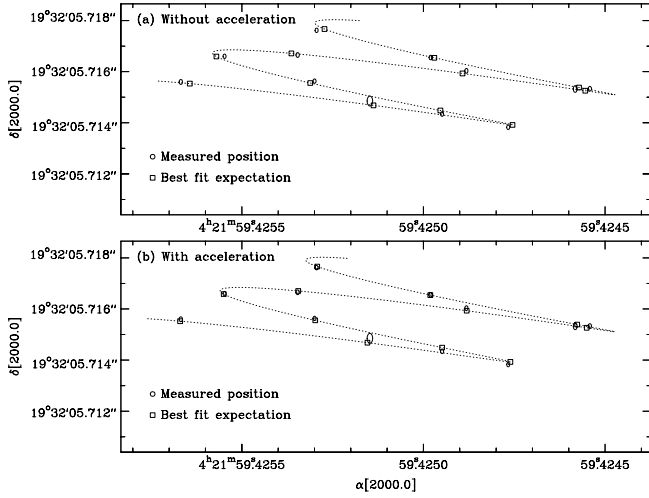


FIG. 1.— Measured positions of T Tau Sb and best fits, both (a) without and (b) with acceleration terms. The observed positions are shown as ellipses, the size of which represents the magnitude of the errors. Note the very significant improvement when acceleration terms are included.

obtained using the SVD method. The reference epoch was taken at the mean of our observations (JD 2453233.586  $\equiv$  J2004.627).

#### 4. RESULTS

The fit to the data points by equations (1) and (2) (Fig. 1a) yields the following astrometric parameters:

$$\begin{aligned}\alpha_{\text{J2004.627}} &= 04^{\text{h}}21^{\text{m}}59.425081^{\text{s}} \pm 0.000005^{\text{s}}, \\ \delta_{\text{J2004.627}} &= 19^{\circ}32'05.71566'' \pm 0.00003'', \\ \mu_{\alpha} \cos \delta &= 4.00 \pm 0.12 \text{ mas yr}^{-1}, \\ \mu_{\delta} &= -1.18 \pm 0.05 \text{ mas yr}^{-1}, \\ \pi &= 6.90 \pm 0.09 \text{ mas}.\end{aligned}$$

This corresponds to a distance of  $145 \pm 2$  pc. The postfit rms, however, is not very good (particularly in right ascension:  $\sim 0.2$  mas), as the fit does not pass through many of the observed positions (Fig. 1a). As a matter of fact,  $75 \mu\text{s}$  and, most notably,  $16.5 \mu\text{s}$  of time had to be added quadratically to the formal errors listed in Table 1 to obtain a reduced  $\chi^2$  of 1 in both right ascension and declination; the errors on the fitted parameters quoted above include this systematic contribution. These large systematic errors most certainly reflect the fact mentioned earlier that the proper motion of T Tau Sb is not uniform because it belongs to a multiple system. Indeed, the fit in which acceleration terms are included is significantly better (Fig. 1b), with a postfit rms of  $60 \mu\text{as}$  in right ascension and  $90 \mu\text{as}$  in declination. It yields the following parameters:

$$\begin{aligned}\alpha_{\text{J2004.627}} &= 04^{\text{h}}21^{\text{m}}59.425065^{\text{s}} \pm 0.000002^{\text{s}}, \\ \delta_{\text{J2004.627}} &= 19^{\circ}32'05.71566'' \pm 0.0004'', \\ \mu_{\alpha, \text{J2004.627}} \cos \delta &= 4.02 \pm 0.03 \text{ mas yr}^{-1}, \\ \mu_{\delta, \text{J2004.627}} &= -1.18 \pm 0.05 \text{ mas yr}^{-1}, \\ a_{\alpha} \cos \delta &= 1.53 \pm 0.13 \text{ mas yr}^{-2}, \\ a_{\delta} &= 0.00 \pm 0.19 \text{ mas yr}^{-2}, \\ \pi &= 6.82 \pm 0.03 \text{ mas}.\end{aligned}$$

To obtain a reduced  $\chi^2$  of 1 in both right ascension and declination, one must add quadratically  $3.8 \mu\text{s}$  of time and  $75 \mu\text{as}$  to

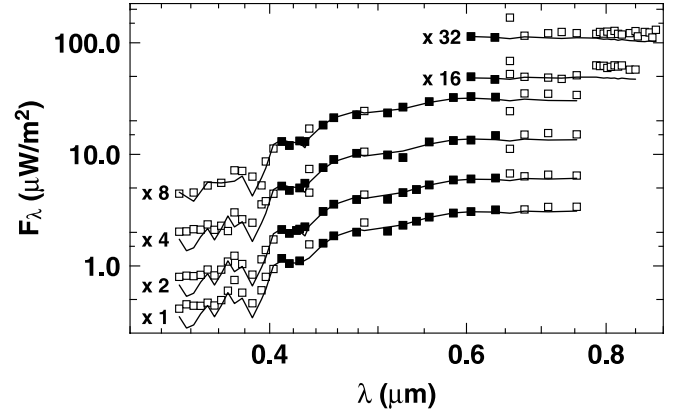


FIG. 2.— Fit to the photometry at six different epochs. Filled squares indicate points that have been fitted; open squares represent other wavelengths that were excluded from the fit.

the statistical errors listed in Table 1. The uncertainties reported above and in the rest of this article include this systematic contribution. Note also that the reduced  $\chi^2$  for the fit without acceleration terms is almost 8 if the latter systematic errors (rather than those mentioned earlier) are used.

The trigonometric parallax obtained when acceleration terms are included corresponds to a distance of  $146.7 \pm 0.6$  pc, which is somewhat larger than, but consistent within  $1.5 \sigma$  of, the value reported by Loinard et al. (2005). Recall, however, that this 2005 result was based on data that had been corrupted by a problem in the VLBA correlator; we consider the present value to be significantly more reliable. The present distance determination is somewhat smaller than, but within  $1 \sigma$  of, the distance obtained by *Hipparcos* ( $d = 177^{+68}_{-39}$  pc). Note that the relative error of our distance is about 0.4%, against nearly 30% for the *Hipparcos* result, a gain of almost 2 orders of magnitude.

#### 5. IMPLICATIONS FOR THE PROPERTIES OF THE STARS

Having obtained an improved distance estimate to the T Tauri system, we are now in a position to refine the determination of the intrinsic properties of each of the components of that system. Since the orbital motion between T Tau N and T Tau S is not yet known to very good precision, we will use synthetic spectra fitting to obtain the properties of T Tau N. For the very obscured T Tau S companion, on the other hand, we will refine the mass determinations on the basis of the orbital fit obtained by Duchêne et al. (2006).

##### 5.1. T Tau N

The stellar parameters ( $T_{\text{eff}}$  and  $L_{\text{bol}}$ ) of T Tau N were obtained by fitting synthetic spectra (Lejeune et al. 1997) to the optical part of the spectral energy distribution. In the absence of recently published optical spectra with absolute flux calibration, we decided to use narrowband photometry taken at six different epochs from 1965 to 1970 (Kuhi 1974). In order to eliminate the contamination by the UV/blue (magnetospheric accretion) and red/IR (circumstellar disk) excesses, we restricted the fit to the range  $0.41\text{--}0.65 \mu\text{m}$ . Two points at  $0.4340$  and  $0.4861 \mu\text{m}$  display large variations between epochs, and these were also discarded, as they are likely to be contaminated by emission lines. As a consequence, 56 photometric measurements at 13 wavelengths and six epochs had to be fitted (see Fig. 2). We assumed that the star had constant intrinsic parameters over the 5 yr of observation, but we allowed the circumstellar extinction to vary.

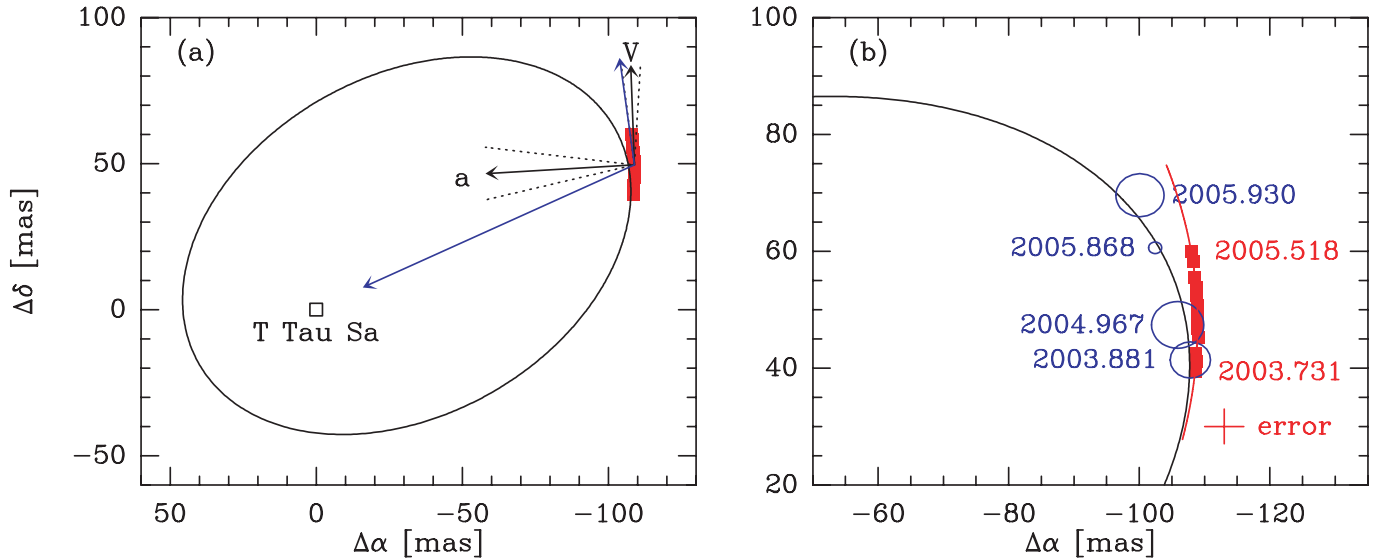


FIG. 3.— (a) VLBA positions (red squares) registered to T Tau Sa, superimposed on the elliptical fit proposed by Duchêne et al. (2006). Also shown are the velocity and acceleration vectors for our mean epoch that we deduced from our observations, as well as their counterparts from the fit by Duchêne et al. (2006; blue arrows). The dotted black lines around the measured acceleration and velocity show the error cones on the direction of each of these vectors. (b) Zoom on the region corresponding to our observations. In addition to the orbit and the VLBA positions, we show our best parabolic fit to our positions (red curve), as well as several recent infrared positions (blue ellipses). The 2003.881 position is from Duchêne et al. (2005), the 2004.967 and 2005.868 positions are from Duchêne et al. (2006), and the 2005.930 position is from Schaefer et al. (2006).

Such an hypothesis is supported by long-term photometric observations (1986–2003) that show color-magnitude diagrams of T Tau elongated along the extinction direction (Mel’nikov & Grankin 2005); Kuhi (1974) also measured significant extinction variation in the period 1965–1970, using color excesses.

The nonlinear fitting procedure used the Levenberg-Marquardt method, and the determination of errors was done using a Monte Carlo simulation. The synthetic spectra were transformed into narrowband photometry by integration over the bandwidth of the measurements (typically  $0.05 \mu\text{m}$ ). As the fitting procedure could not constrain the metallicity, we assumed a solar one. Several fits using randomly chosen initial guesses for  $T_{\text{eff}}$ ,  $L_{\text{bol}}$ , and extinctions were performed in order to ensure that a global minimum  $\chi^2$  was indeed reached. The errors reported by Kuhi (1974; 1.2%) had to be renormalized to 5.9% in order to achieve a reduced  $\chi^2$  of 1. This could result from an underestimation by the author or from positive and negative contamination by spectral lines; indeed, Gahm (1970) reports contamination as high as 20% for RW Aur. The best least-squares fit is represented in Figure 3, and it yields  $T_{\text{eff}} = 5112^{+99}_{-97}$  K and  $L_{\text{bol}} = 5.11^{+0.76}_{-0.66} L_{\odot}$ . The extinction varies between 1.02 and 1.34, within  $1 \sigma$  of the values determined by Kuhi (1974) from color excesses. The effective temperature is consistent with a K1 star, as reported by Kuhi (1974).

In order to derive the age and mass of T Tau N, pre-main-sequence isochrones by D’Antona & Mazzitelli (1996) and Siess et al. (2000) were used. The fitting procedure was identical to the previous one: the age and mass were converted into effective temperature and luminosity, which in turn were converted into narrowband photometry using the synthetic spectra. The derived parameters are shown in Table 3. The masses ( $1.83^{+0.20}_{-0.16}$  and  $2.14^{+0.11}_{-0.10} M_{\odot}$ ) have overlapping error bars and are consistent with values found in the literature (e.g., Duchêne et al. 2006). The predicted ages, on the other hand, differ by a factor of 2. While the isochrones by D’Antona & Mazzitelli (1996) give an age in the commonly accepted range ( $1.15^{+0.18}_{-0.16}$  Myr), a somewhat larger value ( $2.39^{+0.31}_{-0.27}$ ) is derived from those of Siess et al.

(2000). Note that the errors on the derived parameters are entirely dominated by the modeling errors; the uncertainty on the distance now represents a very small fraction of the error budget.

## 5.2. T Tau S

The two members of the T Tau S system have been studied in detail by Duchêne and coworkers in a series of recent articles (Duchêne et al. 2002, 2005, 2006). The most massive member of the system (T Tau Sa) belongs to the mysterious class of “infrared companions” and is presumably the precursor of an intermediate-mass star. T Tau Sb, on the other hand, is a very obscured but otherwise normal pre-main-sequence M1 star. The masses of both T Tau Sa and T Tau Sb were estimated by Duchêne et al. (2006), using a fit to their orbital paths. Those authors used the distance to T Tauri that was deduced by Loinard et al. (2005). Using the new distance determination obtained here, we can renormalize those masses. We obtain  $M_{\text{Sa}} = 3.10 \pm 0.34 M_{\odot}$  and  $M_{\text{Sb}} = 0.69 \pm 0.18 M_{\odot}$ . These values may need to

TABLE 3  
PARAMETERS OF T TAURI N

Parameter	Value
Age (Myr).....	$2.39^{+0.31}_{-0.27}$ (Siess et al. 2000)
	$1.15^{+0.18}_{-0.16}$ (D’Antona & Mazzitelli 1996)
Mass ( $M_{\odot}$ ).....	$2.14^{+0.11}_{-0.10}$ (Siess et al. 2000)
	$1.83^{+0.20}_{-0.16}$ (D’Antona & Mazzitelli 1996)
$T_{\text{eff}}$ (K).....	$5112^{+99}_{-97}$
$L_{\text{bol}}$ ( $L_{\odot}$ ).....	$5.11^{+0.76}_{-0.66}$
$R_{\star}$ ( $R_{\odot}$ ).....	$2.89^{+0.24}_{-0.21}$
$A_V$ , MJD 39095.2.....	$1.34 \pm 0.17$
$A_V$ , MJD 39153.2.....	$1.37 \pm 0.17$
$A_V$ , MJD 39476.3.....	$1.20 \pm 0.17$
$A_V$ , MJD 40869.4.....	$1.02 \pm 0.17$
$A_V$ , MJD 39485.1.....	$1.36 \pm 0.19$
$A_V$ , MJD 39524.1.....	$1.16 \pm 0.19$

be adjusted somewhat, however, as the fit to the orbital path of the T Tau Sa/T Tau Sb system is improved (see below). Note, finally, that the main sources of errors on the masses are related to the orbital motion modeling rather than to the uncertainties of the distance.

## 6. IMPLICATIONS FOR THE ORBITAL MOTIONS

T Tau Sb is a member of a multiple system, so it would be desirable to give its position and express its motion relative to the other members of the system: T Tau N and, particularly, T Tau Sa. Since only T Tau Sb is detected in our VLBA observations, however, registering the positions reported here to the other members of the system involves a number of steps. The absolute position and proper motion of T Tau N has been measured to great precision using over 20 years of VLA observations (Loinard et al. 2003), so registering the position and motion of T Tau Sb relative to T Tau N is fairly straightforward. Combining the data used by Loinard et al. (2003) with several more recent VLA observations, we obtained the following absolute position (at epoch J2000.0) and proper motion for T Tau N:

$$\begin{aligned}\alpha_{J2000.0} &= 04^{\text{h}}21^{\text{m}}59.4321^{\text{s}} \pm 0.0001^{\text{s}}, \\ \delta_{J2000.0} &= 19^{\circ}32'06.419'' \pm 0.002'', \\ \mu_{\alpha} \cos \delta &= 12.35 \pm 0.04 \text{ mas yr}^{-1}, \\ \mu_{\delta} &= -12.80 \pm 0.06 \text{ mas yr}^{-1}.\end{aligned}$$

Subtracting these values from the absolute positions and proper motion of T Tau Sb, we can obtain the positional offset between T Tau Sb and T Tau N, as well as their relative proper motion. For the median epoch of our observations, we obtain

$$\begin{aligned}(\mu_{\alpha} \cos \delta)(\text{Sb/N}) &= -8.33 \pm 0.07 \text{ mas yr}^{-1}, \\ \mu_{\delta}(\text{Sb/N}) &= +11.62 \pm 0.11 \text{ mas yr}^{-1}.\end{aligned}$$

The second step consists of registering the position and motion of T Tau Sb to the center of mass of T Tau S, using the parabolic fits provided by Duchêne et al. (2006). Here both the proper motion and the acceleration must be taken into account. For the mean epoch of our observations, we obtain

$$\begin{aligned}(\mu_{\alpha} \cos \delta)(\text{Sb/CM}) &= +0.3 \pm 0.9 \text{ mas yr}^{-1}, \\ \mu_{\delta}(\text{Sb/CM}) &= +9.3 \pm 0.8 \text{ mas yr}^{-1}, \\ (a_{\alpha} \cos \delta)(\text{Sb/CM}) &= +1.4 \pm 0.2 \text{ mas yr}^{-2}, \\ a_{\delta}(\text{Sb/CM}) &= -0.1 \pm 0.3 \text{ mas yr}^{-2}.\end{aligned}$$

The last correction to be made is the registration of the positions, proper motions, and accelerations to T Tau Sa, rather than to the center of mass of T Tau S. This is obtained by simply multiplying the values above by the ratio of the total mass of T Tau S (i.e.,  $M_{\text{Sa}} + M_{\text{Sb}}$ ) to the mass of T Tau Sa. Using the masses given by Duchêne et al. (2006), we obtain

$$\begin{aligned}(\mu_{\alpha} \cos \delta)(\text{Sb/Sa}) &= +0.4 \pm 1.1 \text{ mas yr}^{-1}, \\ \mu_{\delta}(\text{Sb/Sa}) &= +11.4 \pm 1.0 \text{ mas yr}^{-1}, \\ (a_{\alpha} \cos \delta)(\text{Sb/Sa}) &= +1.7 \pm 0.2 \text{ mas yr}^{-2}, \\ a_{\delta}(\text{Sb/Sa}) &= -0.1 \pm 0.3 \text{ mas yr}^{-2}.\end{aligned}$$

These two vectors are shown in Figure 3, together with the VLBA positions registered to T Tau Sa, several recent infrared ob-

servations, and the elliptical fit obtained by Duchêne et al. (2006). The final error on the VLBA positions is the combination of the original uncertainty on their measured absolute position and of the errors made at each of the steps described above. The final uncertainty is about 3 mas in both right ascension and declination and is shown near the bottom right corner of Figure 3b.

Given the uncertainties, the position of the VLBA source is generally in good agreement with the infrared source position measured at similar epochs. Indeed, the first two VLBA observations were obtained at almost exactly the same time as the infrared image published by Duchêne et al. (2005), and these positions match exactly. The position of the VLBA source at the end of 2004 is also in agreement within  $1 \sigma$  with the position of the infrared source at the same epoch reported by Duchêne et al. (2006). The situation at the end of 2005, however, is somewhat less clear. Extrapolating from the last VLBA observation ( $\sim 2005.5$ ) to the end of 2005 gives a location that would be in reasonable agreement with the position given by Schaefer et al. (2006), but clearly not in agreement with the position obtained by Duchêne et al. (2006). Note, indeed, that the two infrared positions are only very marginally consistent with one another.

Our VLBA observations suggest that T Tau Sb passed the westernmost point of its orbit at around 2005.0, whereas according to the fit proposed by Duchêne et al. (2006), this westernmost position was reached slightly before 2004.0. As a consequence, the trajectory described by the VLBA source is on average almost exactly north-south, whereas according to the fit proposed by Duchêne et al. (2006), T Tau Sb is already moving back toward the east (Fig. 3). We note, however, that the fit proposed by Duchêne et al. (2006; which gives an orbital period of  $21.7 \pm 0.9$  yr) is very strongly constrained by their 2005.9 observation. Schaefer et al. (2006), who measured a position at the end of 2005 that was somewhat further to the north (in better agreement with our VLBA positions), argue that they cannot discriminate between orbital periods of 20, 30, or 40 yr. Orbits with longer periods bend back toward the east somewhat later (see Fig. 10 in Schaefer et al. 2006) and would be in better agreement with our VLBA positions.

Another element that favors a somewhat longer orbital period is the acceleration measured here. According to the fit proposed by Duchêne et al. (2006), the expected transverse proper motion and acceleration are (G. Duchêne 2007, private communication)

$$\begin{aligned}(\mu_{\alpha} \cos \delta)(\text{Sb/Sa}) &= +1.7 \pm 0.2 \text{ mas yr}^{-1}, \\ \mu_{\delta}(\text{Sb/Sa}) &= +12.1 \pm 1.2 \text{ mas yr}^{-1}, \\ (a_{\alpha} \cos \delta)(\text{Sb/Sa}) &= +3.1 \pm 0.5 \text{ mas yr}^{-2}, \\ a_{\delta}(\text{Sb/Sa}) &= -1.4 \pm 0.2 \text{ mas yr}^{-2}.\end{aligned}$$

Thus, while the expected and observed proper motions are in good agreement, the expected acceleration is significantly larger than the observed value (see also Fig. 3). A smaller value of the acceleration would be consistent with a somewhat longer orbital period.

In summary, our observations appear to be in reasonable agreement with all the published infrared positions obtained over the last few years, except for the 2005.9 observation reported by Duchêne et al. (2006). As a consequence, our data favor an orbital period somewhat longer than that obtained by Duchêne et al. (2006). Exactly how much longer is difficult to assess for the following reason. The orbit proposed by Duchêne et al. (2006) was obtained by fitting the observed positions *simultaneously* with a superposition of an elliptical path (of T Tau Sb around

T Tau Sa) and a parabolic trajectory (of T Tau Sa around T Tau N). As a consequence, a modification of the T Tau Sa/T Tau Sb elliptical orbit (as may be required by our data) will result in a change in the parameters of the parabolic fit. But we use the latter to register our VLBA positions, proper motions, and accelerations against T Tau Sa. Thus, an entirely new fit will be needed in order to take into account the present VLBA observations. Such a fit will be presented in a forthcoming paper, in which the numerous VLA observations available from the literature, as well as the VLBI observation from Smith et al. (2003), will also be taken into account.

## 7. CONCLUSIONS AND PERSPECTIVES

Using a series of 12 radio-continuum VLBA observations of T Tau Sb that were obtained roughly every 2 months between 2003 September and 2005 July, we have measured the trigonometric parallax and characterized the proper motion of this member of the T Tauri multiple system with unprecedented accuracy. The distance to T Tau Sb was found to be  $146.7 \pm 0.6$  pc, which is somewhat larger than the canonical value of 140 pc that has

been traditionally used. Using this precise estimate, we have recalculated the basic parameters of all three members of the system. The VLBA positions are in good agreement with recent infrared positions, but our data seem to favor a somewhat longer orbital period than that recently reported by Duchêne et al. (2006) for the T Tau Sa/T Tau Sb system. Finally, it should be pointed out that if observations similar to those presented here were obtained regularly in the coming 5–10 years, they would greatly help to constrain the orbital path (and, therefore, the mass) of the T Tau Sa/T Tau Sb system.

L. L., R. M. T., L. F. R., and R. A. G. acknowledge the financial support of DGAPA, UNAM, and CONACyT, México. The NRAO is a facility of the National Science Foundation operated under cooperative agreement by Associated Universities, Inc. We are indebted to Gaspard Duchêne for calculating the expected velocity and acceleration from his fit, and for his comments on the manuscript. We also thank the anonymous referee for his/her constructive comments on this paper.

## APPENDIX

### FITTING PROCEDURES

The parameters determined in this article (position at a reference epoch, trigonometric parallax, proper motions, and accelerations) were obtained by minimizing the sum ( $\chi_\alpha^2 + \chi_\delta^2$ ) of the residuals in right ascension and declination. The corresponding general mathematical problem is that when two functions  $x$  and  $y$  depend linearly on  $N$  independent parameters ( $a_i$  and  $b_i$  for  $x$  and  $y$ , respectively) and  $M$  common parameters  $c_i$ ,

$$\begin{aligned} x(t) &= \sum_{i=1}^N a_i u_i(t) + \sum_{j=1}^M c_j w_j^x(t), \\ y(t) &= \sum_{i=1}^N b_i v_i(t) + \sum_{j=1}^M c_j w_j^y(t). \end{aligned}$$

The values  $x_k$  and  $y_k$  of the functions  $x$  and  $y$  have been measured at  $P$  epochs,  $t_k$ , with errors  $\sigma_k^x$  and  $\sigma_k^y$ , respectively, and the total  $\chi^2$  can be written as

$$\begin{aligned} \chi^2 &= \chi_x^2 + \chi_y^2 \\ &= \sum_{k=1}^P \left( \left\{ \frac{x_k - \left[ \sum_{i=1}^N a_i u_i(t_k) + \sum_{j=1}^M c_j w_j^x(t_k) \right]}{\sigma_k^x} \right\}^2 + \left\{ \frac{y_k - \left[ \sum_{i=1}^N b_i v_i(t_k) + \sum_{j=1}^M c_j w_j^y(t_k) \right]}{\sigma_k^y} \right\}^2 \right). \end{aligned} \quad (\text{A1})$$

Defining the following matrix elements,

$$\begin{aligned} \alpha_{ki} &= \frac{u_i(t_k)}{\sigma_k^x}, & \beta_{ki} &= \frac{v_i(t_k)}{\sigma_k^y}, \\ \gamma_{kj} &= \frac{w_j^x(t_k)}{\sigma_k^x}, & \delta_{kj} &= \frac{w_j^y(t_k)}{\sigma_k^y}, \\ \theta_k &= \frac{x_k}{\sigma_k^x}, & \psi_k &= \frac{y_k}{\sigma_k^y}, \end{aligned}$$

we can rewrite the total  $\chi^2$  given by equation (A1) as

$$\chi^2 = \sum_{k=1}^P \left[ \left( \theta_k - \sum_{i=1}^N \alpha_{ki} a_i - \sum_{j=1}^M \gamma_{kj} c_j \right)^2 + \left( \psi_k - \sum_{i=1}^N \beta_{ki} b_i - \sum_{j=1}^M \delta_{kj} c_j \right)^2 \right].$$

This sum of quadratic terms can clearly be seen as the squared norm of the vector

$$\begin{pmatrix} \theta_1 - \sum_{i=1}^N \alpha_{1i} a_i - \sum_{j=1}^M \gamma_{1j} c_j \\ \theta_2 - \sum_{i=1}^N \alpha_{2i} a_i - \sum_{j=1}^M \gamma_{2j} c_j \\ \dots \\ \theta_P - \sum_{i=1}^N \alpha_{Pi} a_i - \sum_{j=1}^M \gamma_{Pj} c_j \\ \psi_1 - \sum_{i=1}^N \beta_{1i} b_i - \sum_{j=1}^M \delta_{1j} c_j \\ \psi_2 - \sum_{i=1}^N \beta_{2i} b_i - \sum_{j=1}^M \delta_{2j} c_j \\ \dots \\ \psi_P - \sum_{i=1}^N \beta_{Pi} b_i - \sum_{j=1}^M \delta_{Pj} c_j \end{pmatrix}.$$

Rearranging the terms in this expression, we can rewrite the total  $\chi^2$  as

$$\chi^2 = \left\| \begin{pmatrix} \alpha & 0 & \gamma \\ 0 & \beta & \delta \end{pmatrix} \begin{pmatrix} a \\ b \\ c \end{pmatrix} - \begin{pmatrix} \theta \\ \psi \end{pmatrix} \right\|^2. \quad (\text{A2})$$

The procedure then consists of finding the vector  $\mathbf{X}$  that minimizes an expression of the form

$$\|\mathbf{A}\mathbf{X} - \mathbf{B}\|^2.$$

An efficient algorithm with which to perform this operation is known as singular value decomposition (SVD; see Press et al. 1992). This method is based on the linear algebra theorem that states that any  $I \times J$  rectangular matrix  $\mathbf{M}$  whose number of rows  $I$  is greater than or equal to its number of columns  $J$  can be written as the product of an  $I \times J$  column-orthogonal matrix  $\mathbf{U}$ , a  $J \times J$  diagonal matrix  $\mathbf{W}$  with nonnegative (positive or zero) elements, and the transpose of a  $J \times J$  orthogonal matrix  $\mathbf{V}$ :

$$\mathbf{M} = \mathbf{U}\mathbf{W}\mathbf{V}^T. \quad (\text{A3})$$

The rectangular matrix in equation (A2) has  $2P$  rows (24 in our case) and  $2N + M$  columns (either 5 or 7 for uniform or accelerated proper motions, respectively) and can clearly be decomposed in that fashion. Since both  $\mathbf{U}$  and  $\mathbf{V}$  in the previous expression are orthogonal, their inverses are just their transposes. Also, if none of its diagonal elements are zero (which will be the case in all situations considered here), the inverse of  $\mathbf{W}$  is a diagonal matrix whose elements are just the inverses of those of  $\mathbf{W}$ . Thus, the inverse of matrix  $\mathbf{M}$  can be written as

$$\mathbf{M}^{-1} = \mathbf{V}\mathbf{W}^{-1}\mathbf{U}^T.$$

It can be shown (see Press et al. 1992) that if the matrix  $\mathbf{M}$  can be decomposed as above, then the vector  $\mathbf{X}$  that minimizes the expression  $\|\mathbf{A}\mathbf{X} - \mathbf{B}\|^2$  is simply

$$\mathbf{X} = \mathbf{V}\mathbf{W}^{-1}\mathbf{U}^T\mathbf{B}. \quad (\text{A4})$$

An efficient way of solving our least-squares fitting problem is, therefore, to form the rectangular matrix that appears in equation (A2), decompose it as in equation (A3), and calculate the values of the  $a_i$ ,  $b_i$ , and  $c_i$  using equation (A4). This method was implemented in FORTRAN following Press et al. (1992).

#### REFERENCES

- André, P., Deeney, B. D., Phillips, R. B., & Lestrade, J.-F. 1992, *ApJ*, 401, 667  
 Beasley, A. J., Gordon, D., Peck, A. B., Petrov, L., MacMillan, D. S., Fomalont, E. B., & Ma, C. 2002, *ApJS*, 141, 13  
 Bertout, C., Robichon, N., & Arenou, F. 1999, *A&A*, 352, 574  
 Condon, J. J. 1997, *PASP*, 109, 166  
 D'Antona, F., & Mazzitelli, I. 1996, *ApJ*, 456, 329  
 Duchêne, G., Beust, H., Adjali, F., Konopacky, Q. M., & Ghez, A. M. 2006, *A&A*, 457, L9  
 Duchêne, G., Ghez, A. M., & McCabe, C. 2002, *ApJ*, 568, 771  
 Duchêne, G., Ghez, A. M., McCabe, C., & Ceccarelli, C. 2005, *ApJ*, 628, 832  
 Elias, J. H. 1978a, *ApJ*, 224, 453  
 ———. 1978b, *ApJ*, 224, 857  
 Evans, N. J., II, et al. 2003, *PASP*, 115, 965  
 Feigelson, E. D., & Montmerle, T. 1999, *ARA&A*, 37, 363  
 Fomalont, E. B. 1999, in *ASP Conf. Ser. 180, Synthesis Imaging in Radio Astronomy II*, ed. G. B. Taylor, C. L. Carilli, & R. A. Perley (San Francisco: ASP), 463  
 Gahm, G. F. 1970, *ApJ*, 160, 1117  
 Greisen, E. W. 2003, in *Information Handling in Astronomy*, ed. A. Heck (Dordrecht: Kluwer), 109  
 Güdel, M., et al. 2007, *A&A*, 468, 353  
 Johnston, K. J., Gaume, R. A., Fey, A. L., de Veigt, C., & Claussen, M. J. 2003, *AJ*, 125, 858  
 Kenyon, S. J., Dobrzycka, D., & Hartmann, L. 1994, *AJ*, 108, 1872

- Knude, J., & Høg, E. 1998, *A&A*, 338, 897
- Kuhi, L. V. 1974, *A&AS*, 15, 47
- Lejeune, T., Cuisinier, F., & Buser, R. 1997, *A&AS*, 125, 229
- Loinard, L., Mioduszewski, A. J., Rodríguez, L. F., González, R. A., Rodríguez, M. I., & Torres, R. M. 2005, *ApJ*, 619, L179
- Loinard, L., Rodríguez, L. F., D'Alessio, P., Rodríguez, M. I., & González, R. F. 2007, *ApJ*, 657, 916
- Loinard, L., Rodríguez, L. F., & Rodríguez, M. I. 2003, *ApJ*, 587, L47
- Mel'nikov, S. Y., & Grankin, K. N. 2005, *Astron. Lett.*, 31, 427
- Perryman, M. A. C., et al. 1997, *A&A*, 323, L49
- Phillips, R. B., Lonsdale, C. J., & Feigelson, E. D. 1993, *ApJ*, 403, L43
- Pradel, N., Charlot, P., & Lestrade, J.-F. 2006, *A&A*, 452, 1099
- Press, W. H., Teukolsky, S. A., Vetterling, W. T., & Flannery, B. P. 1992, *Numerical Recipes* (2nd ed.; Cambridge: Cambridge Univ. Press)
- Schaefer, G. H., Simon, M., Beck, T. L., Nelan, E., & Prato, L. 2006, *AJ*, 132, 2618
- Seidelmann, P. K. 1992, *Explanatory Supplement to the Astronomical Almanac* (Mill Valley: University Science Books)
- Siess, L., Dufour, E., & Forestini, M. 2000, *A&A*, 358, 593
- Skinner, S. L., & Brown, A. 1994, *AJ*, 107, 1461
- Smith, K., Pestalozzi, M., Güdel, M., Conway, J., & Benz, A. O. 2003, *A&A*, 406, 957